

# IMAGE ANALYSIS OF ALKALI-AGGREGATE GEL IN CONCRETE PRISM TEST WITH ALKALI-WRAPPING

Go Igarashi<sup>1\*</sup>, Kazuo Yamada<sup>2</sup>, Yanfan Xu<sup>3</sup>, Hong Wong<sup>3</sup>, Shinichi Hirono<sup>4</sup>, Shoichi Ogawa<sup>5</sup>

<sup>1</sup>Tohoku University, Life Cycle Engineering Laboratory, SENDAI, Japan

<sup>2</sup>National Institute for Environmental Studies, Research Center for Material Cycles and Wastes Management, TSUKUBA, Japan

<sup>3</sup>Imperial College, Department of Civil & Environmental Engineering, LONDON, United Kingdom

<sup>4</sup>Taiheiyō Consultant, Analysis Technology Division, SAKURA, Japan

<sup>5</sup>Taiheiyō Consultant, Sales & Marketing Department, TOKYO, Japan

## Abstract

The results from concrete prism test with alkali wrapping (AW-CPT) show complex ASR expansion behaviour that is dependent on temperature and alkali content. In this study, concrete prisms were made with two types of aggregate i.e. rapid expansive andesite containing opal/cristobalite and chert containing chalcedony and cryptocrystalline quartz. ASR was accelerated by increasing the exposure temperature up to 60 °C and alkali content to 5.5 kg/m<sup>3</sup>. An image analysis method was developed to quantify the alkali-silica gel content by treating the samples with uranyl acetate and measuring the emitted fluorescence with a high sensitive camera. Procedures for sample preparation, treatment and imaging were optimized. The results showed that alkali-silica gel inside reactive aggregates may exude out around the reacting aggregate and onto the surface of polished section. A general correlation was observed between the measured ASR gel amount and expansion.

**KEYWORDS:** fluorescent, uranyl acetate, dyeing period, curing period, exposure temperature

## 1 INTRODUCTION

The common approach to prevent alkali-silica-reaction (ASR) is to avoid using reactive aggregates in concrete structures. The level of reactivity of aggregates can be determined using some standardised tests, such as accelerated mortar bar test (ASTM C1260, 1994 [1]) or the concrete prism test (CAN/CSA-A23.2-14A-14, 2014 [2]). However, it is well-known that these and other standard test methods are not always reliable in predicting a given material's ASR-potential. This comes not only from experience with field concrete [4], but also from the intrinsic variability of test results achieved with such standards [2][3]. Thus, in the present study, technologies that enable the identification of ASR characteristics and monitoring of the degree of ASR in concrete structures are investigated.

Visual manifestation of ASR has been summarized by the Federal Aviation Administration [5]. These visual symptoms include laddering, map cracking, aggregate pop-out, reaction rims around aggregate particles, open or gel-filled cracks in aggregate particles, and gel exudation. The structural evidence of expansion due to ASR is also listed – joint closure, seal damage, or misalignment, blow up/heaving [5]. However, visual manifestations of ASR are easily mistaken for other deleterious problems and so cannot be totally relied upon.

In order to accurately diagnose the occurrence of ASR, petrographic analysis with microscopy techniques have been proposed. For example, it has been used to study the presence of cracking and reaction product within and around reactive particles. A procedure is given in AAR-1.1 & 1.2 for the petrographical examination and classification of aggregate samples for AAR potential [6][7]. This procedure enables any potentially alkali-reactive constituents to be identified and, if necessary, quantified [7]. Ben Haha et al. [8] applied image analysis method to measure the degree of ASR from the amount of cracks in the aggregates. In addition to the petrographic analysis, Blight et al. [9] established a scoring system to classify the degree of ASR into five classes based on visual assessment of ASR. Grattan-Bellew and coworkers [10][11][12] developed this scoring system as a damage rating

---

\* correspondence to: [go.igarashi@archi.tohoku.ac.jp](mailto:go.igarashi@archi.tohoku.ac.jp)

index method (DRI). The DRI method is a quantitative method of scoring petrographic features, each of which is weighted to reflect its relative significance in the deterioration process [10][11][12]. However, they identified poor inter-operator consistency among as the primary difficulty, in addition to the excessively time-consuming and tedious nature of the analysis itself [12]. Besides, some methods demand routine access to advanced instrumentation that are not commonly available (e.g. SEM).

In order to simplify the operation and minimize the reliability dependence on operators' judgment, some staining methods have been developed to characterise ASR. Natesaiyer and Hover [13][14] originally put forward a staining method for characterizing ASR gel on concrete surfaces. This staining method relies on uranyl ion ( $\text{UO}_2^{2+}$ ) for gel identification, which fluoresces in green color under shortwave ultraviolet (UV-C) illumination and is found to replace the cation of ASR gel [15][16][17]. After dyeing with uranyl solution, the distribution of deposits of ASR gel appears on concrete surfaces as uranyl ions (green color) under shortwave UV light (UV-C) [13][14]. Guthrie and Carey [18] developed an environmentally friendly method to evaluate alkali-silica reaction. They selected sodium cobaltinitrite ( $\text{Na}_3\text{Co}(\text{NO}_2)_6$ ) and rhodamine B ( $\text{C}_{28}\text{H}_{31}\text{N}_2\text{O}_3\text{Cl}$ ) to stain ASR gel which converts to a pink or yellow color. However, none of these techniques are automated and thus require a lot of time and effort to count and measure the petrographic features of ASR. Rivard et al. [19] further developed the method of Natesaiyer and Hover [13][14] by applying an image analysis software. Livingston et al. [20] also developed another staining method to characterize alkali-silica reaction gel with  $^{40}\text{K}$  or  $^{238}\text{U}$ . Cheng et al. [21] produced and analyzed autoradiographic images with electronic imaging plates. However, this technique does not relate the amount and distribution of ASR gel with the degree of damage. In other words, the reliability of this method has not been verified.

This paper presents a fundamental study to develop a method to quantify ASR gel in concretes containing various amounts of reactive aggregates and alkali contents, and cured under temperatures ranging from 20-60°C. The method is based on fluorescence microscopy and image analysis. In contrast to the use of fractured surfaces such as in the work presented in a previous paper [22], here we used planar sections, which were polished, stained and imaged to quantify the location and amount of the generated ASR gel.

## 2 MATERIALS AND METHODS

### 2.1 Materials, mix designs and concrete prism test (CPT) with alkali wrapping

The specimens used in this study were obtained from specimens that were subjected to ASR concrete prism test (CPT) from two previous papers [23][24]. A brief overview will be provided here. The cement used was ordinary Portland cement (OPC) that conforms to JIS A5211 and CEM I 52.5. The reactive aggregates used were andesite containing opal and cristobalite (N) from Tohoku area, and chert containing chalcedony and cryptocrystalline quartz (T) from Chubu area. A non-reactive limestone aggregate (L) from Kyushu area was also used. Aggregate N is known to show compositional pessimum effect at 30 mass % [25]. Field evidence has shown that Aggregate N causes ASR damage in real structures. However, in the case of Aggregate T, the construction of ASR damaged structure was done several tens of years ago and it was difficult to identify whether the same source of aggregate was used. Nevertheless, it is known that a similar type of chert-containing aggregate is very popular historically and that it is damaging in high alkali cement.

In TABLE 1, details of the specimens from the CPT experiments are shown. In order to assess the influence of temperature, the specimens were cured at 20, 40, or 60 °C. In order to assess the influence of total alkali content in concrete, four levels of alkali content were designed for specimens containing aggregate T from 2.00 to 5.50 kg/m<sup>3</sup> and five levels of alkali content were designed for specimens containing aggregate N from 3.00 to 5.50 kg/m<sup>3</sup>. The specimens were designated according to the following order: aggregate type and ratio – temperature – alkali-content, e.g. N30-60-500 refers to a concrete specimen containing aggregate N at 30 % of total coarse aggregate content by mass, cured at 60 °C, and with an alkali content as  $\text{Na}_2\text{O}_{\text{eq}}$  boosted to 5.00 kg/m<sup>3</sup> by dissolving reagent grade NaOH in the mix water. The water/cement ratio for all specimens was 0.5.

There are several implementations of CPT, however the CSA A23.2 27A-09 and RILEM AAR-3 are considered the most popular and reliable. An accelerated CPT known as RILEM AAR-4 has been published recently [6][26]. In this study, the basic approach of RILEM AAR-3 and AAR-4 [26] was adopted in order to obtain results in shorter time. The size of specimens used was 75×75×250 mm, except for N30-60-550 and N100-60-550, which were 100×100×400 mm according to JASS 5N T603.

The control of alkali leaching and moisture is another important issue for CPT. According to JASS5N-T603, concrete prism is wrapped with wet paper, and the size and the amount of water

needed for wetting are specified. For the 100×100×400 mm prisms, two pieces of unwoven A3 size paper (Kim teck) were used. For each piece of paper, 50 g of water was added. This is important to control moisture condition and to limit alkali leaching [24]. For the smaller specimen 75×75×250 mm, a solution having the same alkali concentration of pore solution of concrete was used instead of water in order to control alkali leaching [24]. After wrapping with wet paper, each specimen was covered by thin PVDC film and was contained in a thick plastic bag in order to prevent the moisture movement between specimen and surrounding environment. Then, four specimens for each experiment level were placed vertically in a container, in which the temperature was controlled with a heater in the bottom of the container, surrounded by heat insulator made of foamed polyurethane board (specimens cured under 20 °C were kept in temperature-controlled room). 24 hours prior to length measurement, specimens were moved to a room at 20 °C. The plastic bag and film, and wrapping paper were removed. Then, the length of the specimen and the mass of wet paper were measured. If necessary, water was added to the same wrapping paper up to the initial mass. The results of expansion behaviour of the specimens were reported by Yamada et al. [23][24], as shown in FIGURE 1 and FIGURE 2.

## 2.2 Methods for assessment and analysis

### *General*

In this paper, three fluorescent observation experiments have been carried out. One was a comparative experiment to determine the influence of alkali content and temperature on ASR, and the other two were experiments to optimize the pre-treatment conditions such as the fluorescent reagent dyeing period and the curing period after surface polishing in order to achieve the optimal contrast of the ASR gel. The fluorescent reagent used was a solution containing uranyl acetate developed by Sanno et al. [27].

### *Photographing technique*

Two high resolution and high sensitivity camera systems were used for the fluorescent observations. The first system was a mirror-less camera (made by SONY, model:  $\alpha$ 7RII, sensor type: 35 mm full-frame CMOS sensor, effective number of pixels: 42.4MP, ISO sensitivity: 50-102 400) and macro lens (made by SONY, model: SEL30M35). The imaging configurations used were as follows: aperture f/22, ISO value 1600, and auto exposure time based on aperture for experiments (1) and (3). The second system used was a mirror-less camera (made by SONY, model: NEX-5N, sensor type: APS-C CMOS sensor, effective number of pixels: 16.1MP, ISO sensitivity: 100-25 600) and single focus lens (made by SONY, model: SEL16F28). The imaging configurations were aperture: f/28, ISO value: 100, and fixed exposure time 30 s, and this was used for experiment (2).

### *Sample preparation*

From the CPT specimens, cross-sections about 20 mm in thickness were obtained perpendicular to the prism axis with a concrete saw. Then, the sections were wet polished with abrasive powder (carborundum – SiC, mesh #400 and #800), and subsequently rinsed in an ultrasonic cleaner with water.

### *Fluorescence observation experiment (1) – influence of curing temperature and alkali content*

The polished sections were wrapped with wet paper and PVDC film for several days as shown in TABLE 1. Then, the PVDC film was removed carefully so as not to disturb the surface of the sections, and subsequently immersed in the treatment solution for approximately 10 minutes to allow ion exchange between ASR gel and uranyl acetate. As mentioned in Section 1, the stained ASR gel is best observed under shortwave ultraviolet illumination to induce a characteristic greenish fluorescence [13][14]. Thus, a shortwave 254 nm ultraviolet (UV-C) [15][16][17] bench lamp was used to illuminate the sample and images were then taken at a regular time interval.

### *Fluorescence observation experiment (2) – dyeing period of fluorescent reagent*

The polished sections were wrapped with wet paper and PVDC film for a week. Then, the sections were unwrapped and immersed in the treatment solution. Pictures were then taken at a regular time interval using the high sensitivity camera in order to determine the time required to allow a complete ion exchange between ASR gel and uranyl acetate. This is established when the ASR gel on the surface showed a saturated fluorescent intensity. Subsequently, the stained sections were removed from the solution and dried. Again, images were then taken at a regular time interval to establish the effect of drying on the detectable gel fluorescence.

### *Fluorescence observation experiment (3) – curing period after polishing surface*

The polished sections were put in a wet box, which was humidified by bubbling de-carbonated water using high pressured N<sub>2</sub> gas. The sections were then brought out and immersed in the treatment solution for 30-40 min. Images were then taken every other day to detect the time required for the ASR gel to seep out from the reacted aggregate particles to the surface.

## **3 RESULTS AND DISCUSSION**

### **3.1 Curing temperature and alkali content**

Figures 3 and 4 show example images of the treated sections captured under normal visible light and 254 nm short-wave UV light (UV-C). The results of quantitative image analysis of the fluorescent area using the software package Image J are summarized in TABLE 1. Finally, the relationship between maximum expansion (at 46 weeks) and the measured fluorescent area is shown in Figure 5.

From FIGURE 3, one can compare the effect of curing temperature and alkali content on the amount of ASR gel in concrete specimens containing aggregate T. On average, the highest amount of ASR gel was observed at a curing temperature of 40°C, followed by curing at 60°C and 20°C. Almost no ASR gel was observed when the specimens were cured at 20°C. Although little influence of the alkali content was noticed, there seems to be a positive correlation between alkali content and amount of ASR gel for the specimens cured at 60°C.

From FIGURE 4, one can compare the effect of curing temperature and alkali content on the amount of ASR gel in concrete specimens containing aggregate N. Interestingly, it was observed that aggregate N produced more ASR gel compared to aggregate T. Although it appears that curing temperature had little influence there seems to be a positive correlation when the results of N30-60-425, N30-40-425 and N30-20-425 are compared. These trends are different from those seen in the specimens containing aggregate T, where the temperature effect on gel amount is obscure. Only for the case of curing at 60°C where higher alkali content resulted in higher fluorescent area.

The correlation between fluorescent area and the maximum expansion at 46 weeks is shown in FIGURE 5. Most of the specimens showed a positive correlation between the amount of detected ASR gel and expansion, apart from the specimens containing aggregate N that were cured at 20°C. It should be noted here that specimens N30-40-300, N30-20-550, N30-20-300 and N30-20-250 were wrapped longer than the other specimens (see TABLE 1). Therefore, the lack of correlation observed for the specimens cured at 20°C seems to be a result of the difference in wrapping period after polishing.

In conclusion, the amount of fluorescence observed on the treated specimens is a good indicator for evaluating the amount of ASR gel in concretes containing reactive aggregates. However, it is important to standardize the treatment procedure such as the period of wet wrapping prior to imaging.

### **3.2 Dyeing period of fluorescent reagent**

The effect of immersion time in uranyl acetate solution on the development of ASR gel fluorescence is shown in FIGURE 6. It can be seen that the amount of detectable fluorescence on the surface of the section gradually increases with increase in immersion time. A significant amount of fluorescence can be observed by around 10 min, however the fluorescence intensity only becomes saturated after an immersion period of 30 min.

Once the ASR gel on the surface showed saturated fluorescence intensity, the specimen was dried and the effect of drying time on subsequent change in fluorescence intensity is shown in FIGURE 7. Note that the written time in FIGURE 7 is the time after immersion in the uranyl acetate solution and the values in brackets is the amount of time spent on drying the specimen. It can be observed from FIGURE 7, that the area of fluorescence does not seem to change, but the intensity of the fluorescence appears to increase with drying time.

In conclusion, it is important to immerse the specimen in uranyl acetate solution for at least 30 min and then dry the specimen for a sufficient amount of time in order to obtain a high amount of fluorescence intensity to detect the ASR gel.

### **3.3 Curing period after polishing surface**

FIGURE 8 presents a series of images of the same specimen captured at various times showing the exudation of ASR gel onto the specimen surface when placed in a high humidity box. ASR gel was not observed initially, but it gradually seeps out onto the surface of the cross-section from reactive

aggregate particles and becomes saturated after a week. This suggests that all ASR gel observed in the section originally were washed out during the wet sawing process. As such, the ASR gel observed on the surface of cores drilled out from concrete structures in wet condition would not be located in the original condition due to exudation from reactive aggregates in the section. To provide further evidence of this, FIGURE 9 shows a fractured cross-section stained with uranyl acetate solution for 10 min that was imaged immediately after splitting. The figure shows significant amounts of fluorescent ASR gel present in the cement paste matrix and air voids. However, very little ASR gel was observed in reactive aggregates compared to the case when the specimen was kept in wet condition for several days. In conclusion, keeping specimens in a wet condition for some days after polishing will induce fluorescence on the reactive aggregates due to exudation of the ASR gel.

#### 4 CONCLUSIONS

In this paper, the potential of uranyl acetate staining combined with fluorescent imaging and wet wrapping method for testing the degree of ASR in concrete cross-sections was investigated. The main observations are as follows:

- The overall fluorescent area correlates well with the presence of ASR gel on polished sections, and with the amount of expansion of the concrete prism;
- At least 30 min is required to stain the ASR gel to achieve saturation in fluorescence intensity and care must be taken during drying to prevent loss of ASR gel;
- ASR gel will gradually seep out from sliced/polished reactive aggregates and cover the surface around them in wet conditions;
- A wet type procedure enables the observation of ASR gel in the reactive aggregates.

Furthermore, it is recommended to use a high-quality imaging system to capture fluorescent images as this can significantly help in detecting the ASR gel and reactive aggregates. However, more work needs to be done to further optimise the method for detecting and measuring the exuded ASR gel in cement paste matrix. In conclusion, the current method is useful for detecting ASR gel in reactive aggregates and its application will facilitate research on ASR mechanism and deterioration diagnosis for concrete structures.

#### 5 ACKNOWLEDGEMENT

Concrete specimens used in this study have been prepared by Kyushu University. The authors thank to Mr. Akihiro Tanaka, Mr. Daisuke Yamamoto of a technician and associated professor Yasutaka Sagawa of Kyushu University.

#### 6 REFERENCES

- [1] ASTM C1260. (1994): Standard Test Method for Potential Alkali Reactivity of Aggregates (Mortar-Bar Method), ASTM International, West Conshohocken, PA.
- [2] CAN/CSA-A23.2-14A-14. (2014): Potential Expansivity of Aggregates; Procedure for Length Change Due to Alkali-Aggregate Reaction in Concrete Prisms. Canada, CSA.
- [3] ASTM C289-07. (2007): Standard Test Method for Potential Alkali-Silica Reactivity of Aggregates (Chemical Method). West Conshohocken, PA, ASTM international.
- [4] Bérubé, M, and Fournier, B (1993): Canadian experience with testing for alkali-aggregate reactivity in concrete. *Cement and Concrete Composites*. 15 (1), 27-47.
- [5] Sarkar, S, Zollinger, D, Mukhopadhyay, A, Lim, S, and Shon, C (2004): Handbook for identification of alkali-silica reactivity in airfield pavements. US Department of Transportation, Federal Aviation Administration, AC No150/5380-8 Appendix. 1.
- [6] RILEM (2016): RILEM Recommended Test Method: AAR-0 – Outline guide to the use of RILEM methods in the assessment of the alkali-reactivity potential of aggregates. In: Nixon, PJ, and Sims, I (editors): RILEM recommendations for the prevention of damage by alkali-aggregate reactions in new concrete structures. Springer Verlag, Heidelberg-Berlin/DE. RILEM State-of-the-art Report (17): 5-34.
- [7] RILEM (2016): RILEM Recommended Test Method: AAR-1.1 – Detection of potential alkali-reactivity – Part 1: Petrographic examination method. In: Nixon, PJ, and Sims, I (editors): RILEM recommendations for the prevention of damage by alkali-aggregate reactions in new concrete structures. Springer Verlag, Heidelberg-Berlin/DE. RILEM State-of-the-art Report (17): 35-60.
- [8] Ben Haha, M, and Gallucci, E, Guidoum, A, and Scrivener, KL (2007): Relation of expansion due to alkali silica reaction to the degree of reaction measured by SEM image analysis. *Cement and Concrete Research*. 37 (8), 1206-1214.

- [9] Blight, G, McIver, J, Schutte, W, and Rimmer, R (1981): The effects of alkali-aggregate reaction on reinforced concrete structures made with Witwatersrand quartzite aggregate. Proceedings of the 5<sup>th</sup> International Conference on Alkali-Aggregate Reaction in Concrete - ICAAR.
- [10] Grattan-Bellew, PE, and Danay, A (1992): Comparison of laboratory and field evaluation of AAR in large dams. Proceedings of the International Conference on Concrete AAR in Hydroelectric Plants and Dams, Canadian Electrical Association (CEA), Montréal, in association with Canadian National Committee of the International Committee on Large Dams (ICOLD), Fredericton, Canada: pp23.
- [11] Dunbar, PA, Grattan-Bellew, PE (1995): Results of damage rating evaluation of condition of concrete from a number of structures affected by ASR. CANMET/ACI International Workshop on Alkali-Aggregate Reactions in Concrete, Dartmouth, Canada, October: 257-266.
- [12] Grattan-Bellew, P, and Mitchell, LB (2006): Quantitative petrographic analysis of concrete - the damage rating index (DRI) method, a review. In: Fournier, B (editor): Marc-André Bérubé Symposium on alkali-aggregate reactivity in concrete. 8th CANMET/ACI International Conference on Recent Advances in Concrete Technology, May 31 - June 3, 2006, Montréal, Canada: 321-334.
- [13] Natesaiyer, K, and Hover, K (1988): In-situ identification of ASR products in concrete. Cement and Concrete Research. 18 (3), 455-463.
- [14] Natesaiyer, K, and Hover, KC (1989): Further study of an in-situ identification method for alkali-silica reaction products in concrete. Cement and Concrete Research (19): 770-778.
- [15] Ahrlund, S, Grenthe, I, and Noren, B (1960): The ion exchange properties of silica gel. I – The sorption of Na<sup>+</sup>, Ca<sup>2+</sup>, Ba<sup>2+</sup>, UO<sub>2</sub><sup>2+</sup>, Gd<sup>3+</sup>, Zr(IV)+Nb, U(IV) and Pu(IV). Acta Chemica Scandinavia. 14, 1059-1076.
- [16] Traverso, O, Carassiti, V, Portanova, R, and Vigato, PA (1974): Photochemical reactions of uranyl complexes. Dipyrindine uranyl nitrate. Inorganica Chimica Acta (9): 227-230.
- [17] Gorobets, BS, and Rogojine, AA (2002): Luminescent spectra of minerals. Reference book. All-Russia Scientific Research Institute of Mineral Resources, Moscow: pp300
- [18] Guthrie, GD, and Carey, JW (1997): A simple environmentally friendly, and chemically specific method for the identification and evaluation of the alkali-silica reaction. Cement and Concrete Research. 27 (9), 1407-1417.
- [19] Rivard, P, Fournier, B, and Ballivy, G (2000): Quantitative petrographic technique for concrete damage due to ASR: experimental and application. Cement, Concrete and Aggregates. 22 (1), 63-72.
- [20] Livingston, R, Aderhold, H, Hover, K, Hobbs, S, and Cheng, Y (2000): Autoradiographic methods for identifying alkali-silica reaction gel. Cement, Concrete and Aggregates. 22 (1), 37-40.
- [21] Cheng, Y, Soodprasert, T, and Hutchinson, J (1996): Radioactivity measurements using storage phosphor technology. Applied Radiation and Isotopes. 47 (9), 1023-1031.
- [22] Sangsuwan, C, and Sujjavanich, S (2012): Effects of moderate calcium oxide fly ash on expansion of mortar bar due to Thai reactive aggregates. Engineering Journal 16(3):101-107.
- [23] Yamada, K, Karasuda, S, Ogawa, S, Sagawa, Y, Osako, M, Hamada, H, and Isneini, M (2014): CPT as an evaluation method of concrete mixture for ASR expansion. Construction and Building Materials (64): 184-191.
- [24] Yamada, K, Sagawa, Y, Nagase, T, Ogawa, S, Kawabata, Y, and Tanaka, A (2015): The importance of alkali-wrapping for CPT. In: Proceedings of the 14<sup>th</sup> International Conference on Alkali-Aggregate Reaction in Concrete – ICAAR: (*this volume*).
- [25] Kawabata, Y, Yamada, K, and Matsushita, H (2012): Suppression effect of fly ash on ASR expansion of mortar/concrete at the pessimum proportion. In: Proceedings 13<sup>th</sup> International Conference on Alkali-Aggregate Reaction in Concrete – ICAAR, Austin/TX: 031711-KAWA.
- [26] RILEM (2016): RILEM Recommended Test Method: AAR-4.1 – Detection of potential alkali-reactivity 60 °C test method for aggregate combinations using concrete prisms. In: Nixon, PJ, and Sims, I (editors): RILEM recommendations for the prevention of damage by alkali-aggregate reactions in new concrete structures. Springer Verlag, Heidelberg-Berlin/DE. RILEM State-of-the-art Report (17): 99-116.
- [27] Sanno, C, Maruyama, T, Yamanobe, H, and Torii, K (2013): Development of simple method of ASR diagnosis by gel fluorescence method. Proceedings of Annual Conference of JCI (35): 973-978 (in Japanese).

TABLE 1 Designed level, expansion in CPT and wrapping period before fluorescent test.

Specimen	Coarse aggregate	Temp (°C)	Alkali content (kg/m <sup>3</sup> )	Maximum expansion (% $\ell/\ell$ )	Wrapping period (days)	Fluorescent area (% m <sup>2</sup> /m <sup>2</sup> )	Ref.
T100-60-550	T	60	5.50	0.067	3	24.7	[24]
T100-60-475	T	60	4.75	0.044	4	18.0	[24]
T100-60-400	T	60	4.00	0.039	3	11.4	[24]
T100-60-300	T	60	3.00	0.030	4	10.9	[24]
T100-40-550	T	40	5.50	0.069	4	32.2	[24]
T100-40-475	T	40	4.75	0.065	4	23.2	[24]
T100-40-400	T	40	4.00	0.064	4	30.4	[24]
T100-20-550	T	20	5.50	0.008	3	7.7	[24]
N30-60-550	N: L = 3: 7	60	5.50	0.173	6	35.8	[24]
N30-60-425	N: L = 3: 7	60	4.25	0.162	6	38.4	[24]
N30-60-300	N: L = 3: 7	60	3.00	0.113	3	27.1	[24]
N30-60-250	N: L = 3: 7	60	2.50	0.088	4	24.8	[24]
N30-60-200	N: L = 3: 7	60	2.00	0.061	4	12.8	[24]
N30-40-550	N: L = 3: 7	40	5.50	0.131	3	33.7	[24]
N30-40-425	N: L = 3: 7	40	4.25	0.123	3	38.0	[24]
N30-40-300	N: L = 3: 7	40	3.00	0.143	8	38.7	[24]
N30-20-550	N: L = 3: 7	20	5.50	0.097	8	39.5	[24]
N30-20-425	N: L = 3: 7	20	4.25	0.095	4	24.4	[24]
N30-20-300	N: L = 3: 7	20	3.00	0.096	8	49.0	[24]
N30-20-250	N: L = 3: 7	20	2.50	0.102	8	33.7	[24]
N30-60-550*	N: L = 3: 7	60	5.50	0.208	—	—	[23]
N100-60-550*	N	60	5.50	0.176	—	—	[23]

\* specimen dimensions: 100×100×400 mm.

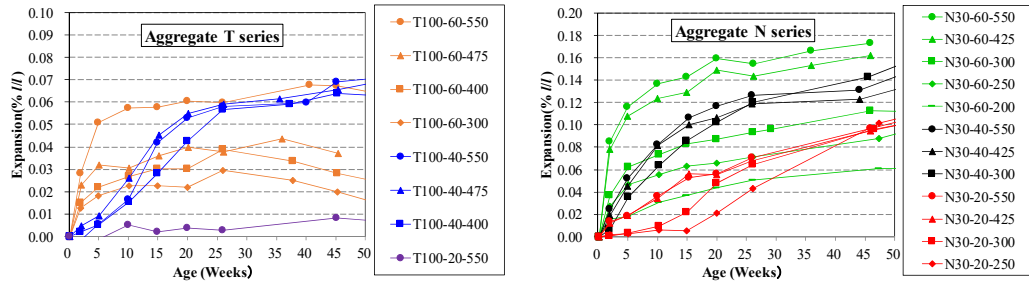


FIGURE 1 Development of uniaxial expansion of concrete prism during CPT (left: aggregate T series, right: aggregate N series).

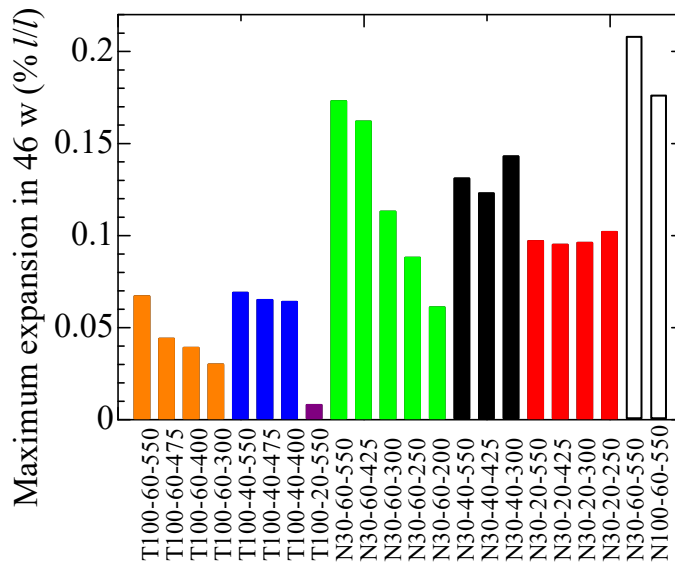


FIGURE 2 Maximum uniaxial expansion of concrete prism during CPT in 46 weeks.

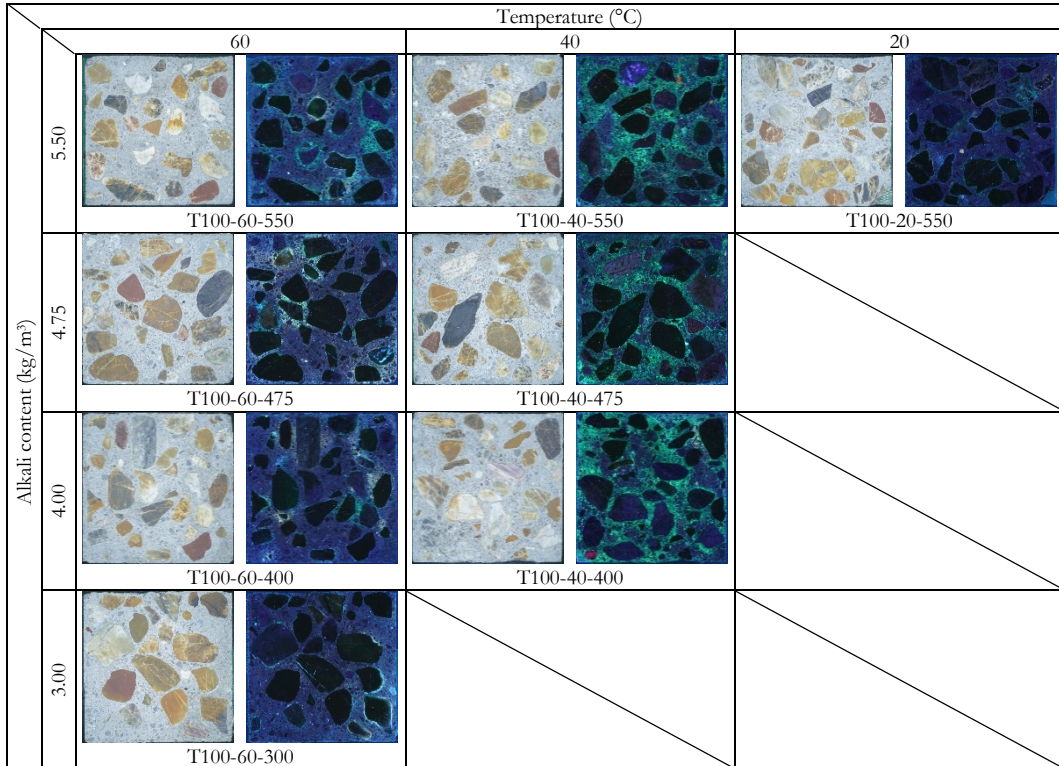


FIGURE 3 ASR gel by fluorescence of T series under visible light (left) and UV-C light (right).

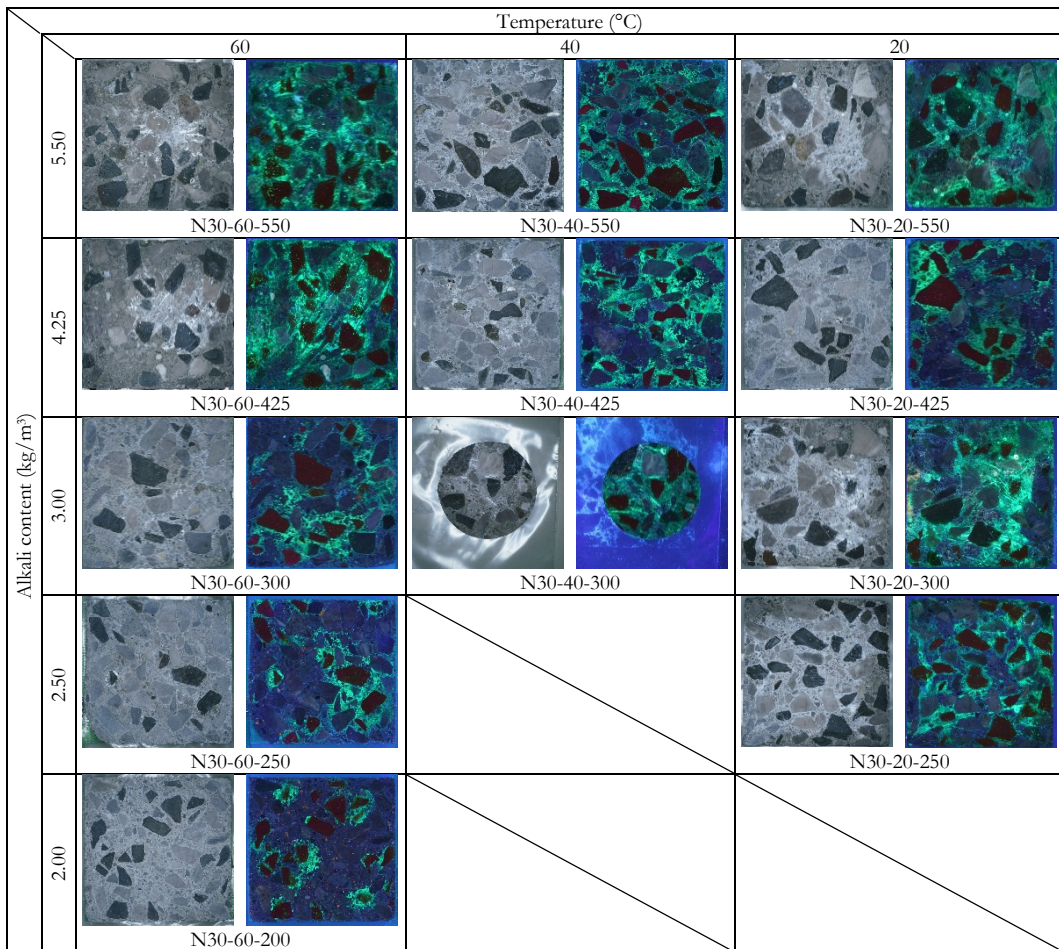


FIGURE 4 ASR gel by fluorescence of N series under visible (left) and UV-C light (right).

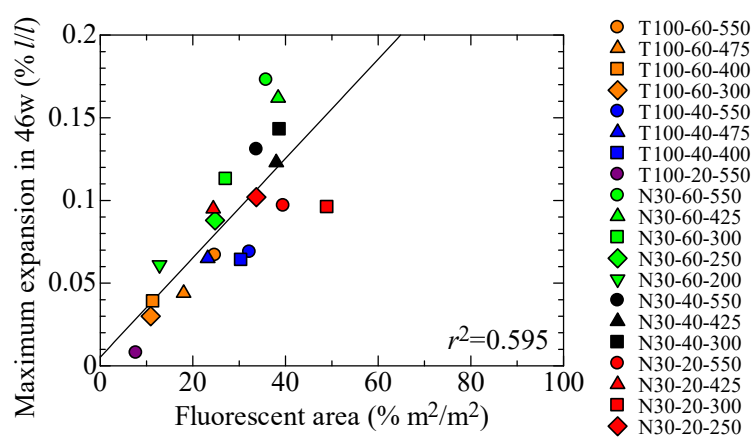


FIGURE 5 Relationship between maximum expansion at 46 weeks and the image measured fluorescent area.

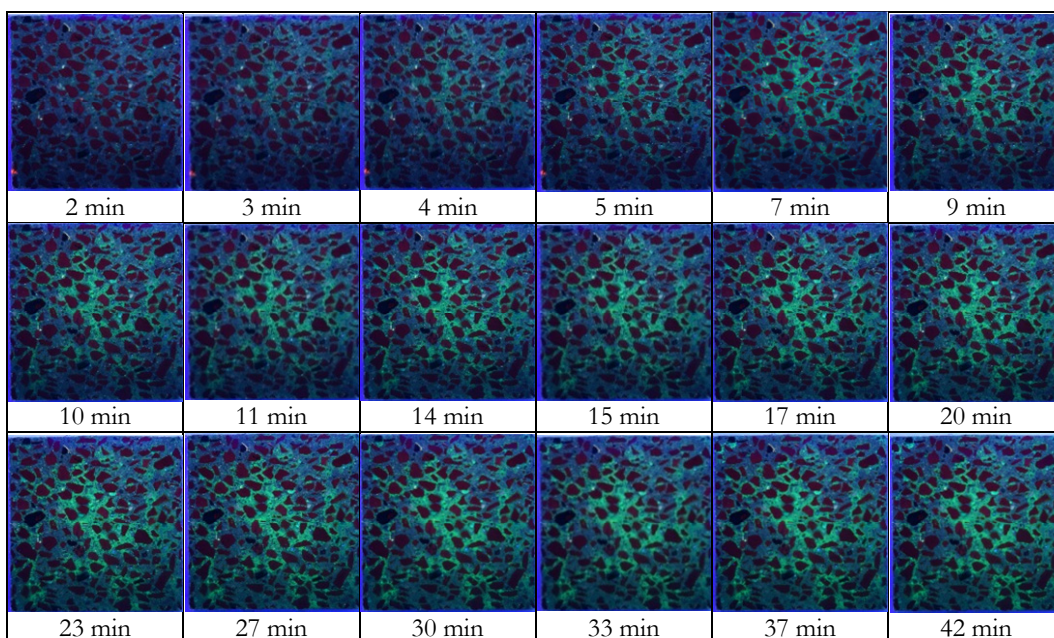


FIGURE 6 Effect of immersion time in uranyl acetate solution on the detectable ASR gel fluorescence.

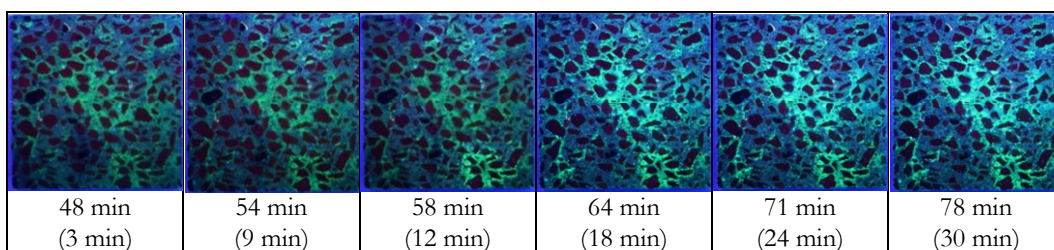


FIGURE 7 Effect of drying time (shown in brackets) on the detectable ASR gel fluorescence intensity.

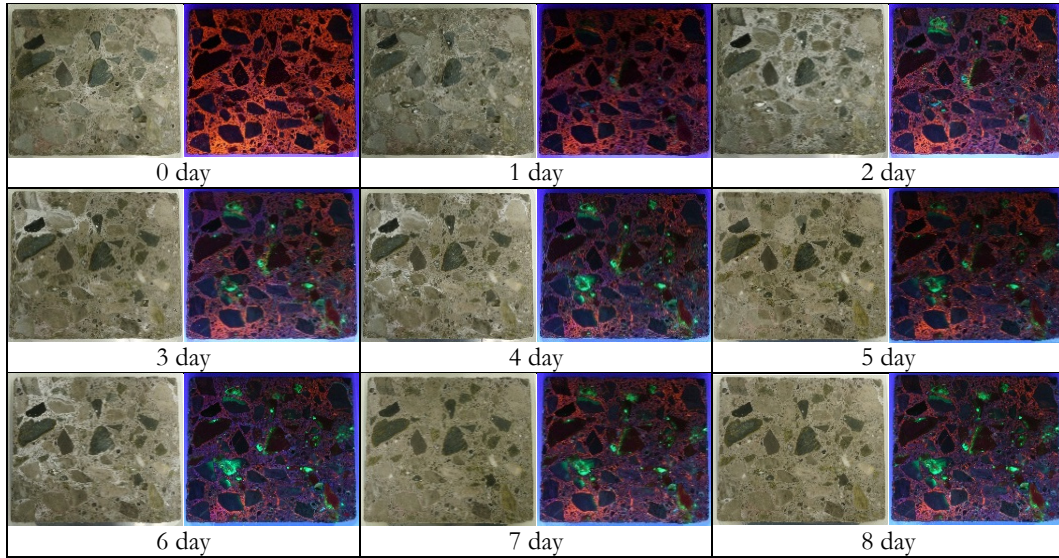


FIGURE 8 Time series images showing the exudation of ASR gel onto the specimen surface in a high humidity box under visible light (left side) and 254 nm wave-length UV light (UV-C) (right side).

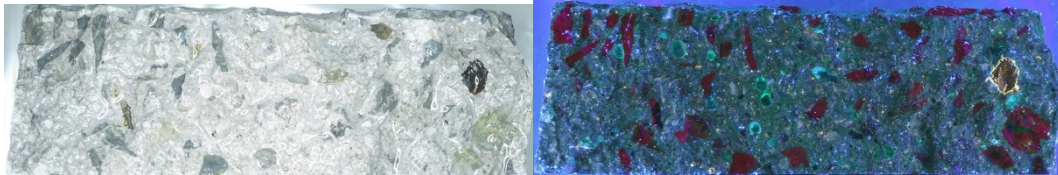


FIGURE 9 ASR gel distribution on a fractured cross-section stained by uranyl acetate solution under visible light (left side) and 254 nm wave-length UV light (UV-C) (right side).